ORIGINAL RESEARCH

# Myocardial Oxygen Consumption and Efficiency in Patients With Cardiac Amyloidosis

Tor Skibsted Clemmensen MD, PhD; Jens Soerensen, MD, DMSc; Nils Henrik Hansson, MD, PhD; Lars Poulsen Tolbod, PhD; Hendrik J. Harms, PhD; Hans Eiskjær, MD, DMSc; Fabian Mikkelsen, MD; Henrik Wiggers, MD, DMSc; Niels Frost Andersen, MD, PhD; Steen Hvitfeldt Poulsen MD, DMSc

***Background*—**This study evaluated myocardial oxygen consumption ($MVO_2$) and myocardial external efficiency (MEE) in patients with cardiac amyloidosis (CA). Furthermore, we compared MEE and $MVO_2$ in subjects with light chain amyloidosis versus transthyretin (ATTR) amyloidosis.

***Methods and Results*—**The study population comprised 40 subjects: 25 patients with confirmed CA and 15 control subjects. All subjects underwent an $^{11}$C-acetate positron emission tomography. Furthermore, the CA patients underwent comprehensive echocardiography and right heart catheterization during a symptom-limited, semi-supine exercise test. MEE was calculated from $^{11}$C-acetate positron emission tomography as the ratio of left ventricular (LV) stroke work and the energy equivalent of $MVO_2$. Myocardial work efficiency was calculated as echocardiography-derived work pressure product divided by three-dimensional LV mass. CA patients had significantly lower LV-ejection fraction (54±13% versus 63±4%, $P<0.05$) and LV-global longitudinal strain (LVGLS) (12±4% versus 19±2%, $P<0.0001$) and a more restrictive filling pattern (E/e′-ratio 18 [12–25] versus 8 [7–9], $P<0.0001$) than controls. MEE was severely reduced (13±5% versus 22±5%, $P<0.0001$) whereas total $MVO_2$ was higher (18±6 mL/min versus 13±3 mL/min, $P<0.01$) in CA patients than controls. MEE decreased with increasing New York Heart Association symptom burden ($P<0.0001$). We found a good relationship between MEE and peak exercise systolic performance (LVGLS: $R^2=0.60$, $P<0.0001$; myocardial work efficiency: $R^2=0.48$, $P<0.0001$; cardiac index: $R^2=0.52$, $P<0.0001$) and between MEE and myocardial blood flow ($R^2=0.44$, $P<0.0001$).

***Conclusion*—**Myocardial oxidative metabolism is disturbed in CA patients with increased total $MVO_2$ and reduced MEE. MEE correlated significantly with echocardiographic derived systolic parameters such as myocardial work efficiency and LVGLS that might be used as surrogate MEE markers. **(*J Am Heart Assoc*. 2018;7:e009974. DOI: 10.1161/JAHA.118.009974.)**

**Key Words:** amyloid • efficiency measures • exercise physiology • myocardial metabolism • myocardial oxygen consumption • positron emission tomography • speckle tracking echocardiography • stress echocardiography

Cardiac amyloidosis (CA) is characterized by concentric biventricular wall thickness because of extracellular deposition of misfolded proteins. The resulting myocardial stiffness eventually leads to heart failure and death.[1–5] However, it has been proposed that the heart failure pathogenesis is multifactorial involving both myocardial structural and vascular damage but also proteotoxicity from light chains, which leads to cellular and mitochondrial dysfunction.[4] The inefficient energy exploitation and mitochondrial dysfunction may play an important role in heart failure development.[6–8] A normal myocyte contractile state is highly dependent on the myocardial energy resources and consumption. Myocardial oxygen consumption ($MVO_2$), as well as myocardial blood flow (MBF), can be measured non-invasively by $^{11}$C-acetate positron emission tomography (PET).[9] Subsequently, the mechanoenergetic coupling can be calculated as myocardial external efficiency (MEE), which reflects the ratio of LV external stroke work (EW) and the energy equivalent of $MVO_2$.[8–11] MEE may provide *as today* unknown important information about myocardial function in CA patients and may benefit in the non-invasive diagnosis[12] and risk stratification of patients with CA.

In the present study, we hypothesized that $MVO_2$ and MEE were key determinants of myocardial contractile and exercise

*From the Departments of Cardiology (T.S.C., N.H.H., H.E., F.M., H.W., S.H.P.) and Nuclear Medicine & PET Center (J.S., L.P.T., H.J.H.), Aarhus University Hospital, Skejby, Aarhus N, Denmark; Department of Haematology, Aarhus University Hospital, Aarhus N, Denmark (N.F.A.).*

**Correspondence to:** Tor Skibsted Clemmensen, MD, PhD, Department of Cardiology, Aarhus University Hospital Skejby, Palle Juul-Jensens Boulevard 99, 8200 Aarhus N, Denmark. E-mail: torclemm@rm.dk

Received June 1, 2018; accepted September 24, 2018.

## Clinical Perspective

### What Is New?

- Myocardial external efficiency is significantly reduced in patients with cardiac amyloidosis and is significantly associated with decreasing systolic myocardial performance.
- Total myocardial oxygen consumption and myocardial external efficiency is abnormal even in cardiac amyloidosis patients in New York Heart Association class I, which indicates that myocardial oxidative metabolism deteriorates prior development of symptoms and therefore the inefficient myocardial energy exploitation and mitochondrial uncoupling may play a central role in the transition to symptomatic heart failure in patients with cardiac amyloidosis.

### What Are the Clinical Implications?

- The reduced myocardial external efficiency may be an important component in the poor myocardial contractility seen in cardiac amyloidosis patients, and non-invasive assessment of systolic myocardial deformation by global longitudinal strain may serve as a surrogate myocardial external efficiency marker in these patients.

capacity in patients with CA. We investigated MEE, MBF, and $MVO_2$ differences in light-chain amyloidosis (AL) and transthyretin amyloidosis patients and compared our findings with subjects without CA.

## Methods

The data, analytic methods, and study materials will not be made available to other researchers for purposes of reproducing the results or replicating the procedure as our local scientific ethical committee have not provided data sharing approval.

## Study Population

We enrolled 35 subjects in the study at the Department of Cardiology, Aarhus University Hospital, Denmark from September 2015 to November 2016. Twenty-five subjects had confirmed CA and 10 subjects served as controls. The CA positive group comprised wild-type transthyretin (ATTRwt) patients (n=10), familial transthyretin amyloidosis mutation carriers (ATTRm) of the Danish ATTRm mutation (Leu111Met) and with cardiac involvement (n=5), and AL patients with cardiac involvement (n=10). CA was confirmed by endomyocardial biopsy using Congo red dye and immunohistochemistry in all but 1 patient. The last patient (ATTRm) was considered to have CA because of a positive $^{11}$C-Pittsburgh compound B (PIB) positron emission tomography (PET)[13–15] even though the patient was not subjected to endomyocardial biopsy. The control group consisted of 10 healthy controls. These healthy controls received no medication, had no cardiopulmonary symptoms, and had normal ECGs. The patients were included from our outpatient clinic. We excluded patients with significant valve disease. Four of the ATTRm patients with cardiac involvement were liver transplanted to postpone the cardiac amyloid progression.

The CA patients underwent both $^{11}$C-acetate PET and exercise stress test with simultaneous right heart catheterization, echocardiography, and oxygen consumption evaluation. The healthy controls underwent $^{11}$C-acetate PET and resting echocardiography.

All participants were aged ≥18 years and were included after having provided written informed consent according to the principles of the Helsinki Declaration. The local scientific ethical committee of the Central Denmark Region approved the study. Echocardiographic and hemodynamic data from these patients has previously been published.[16,17] The $^{11}$C-acetate PET was performed within 3 weeks of exercise stress test.

## $^{11}$C-Acetate Positron Emission Tomography

An $^{11}$C-acetate PET scan was performed in all subjects in the resting state on a Siemens Biograph TruePoint TrueV 64 PET/CT scanner. We placed a catheter in an antecubital vein. The subjects rested for a minimum of 30 minutes. Subsequently, $^{11}$C-acetate (5 MBq/kg) was injected followed by a 27-minute list mode PET recording. The heart rate and arterial blood pressure was measured by sphygmomanometer at 5, 10, and 20 minutes after injection.

Reconstruction of dynamic images was performed as described in a previous paper from our group.[18] The aQuant software package was used for dynamic data sets analysis using automatically obtained image-derived and metabolites-corrected arterial input functions.[19] The average LV time-activity curve was obtained and fitted into a 1-tissue compartment model yielding the global myocardial clearance rate ($k_2$).[20,21] MBF was estimated using the global uptake rate ($K_1$), which was corrected for the incomplete extraction of $^{11}$C-acetate.[22] $MVO_2$ (mL/min per gram) was calculated from $k_2$ as $MVO_2=(135\times k_2-0.96)/100$.[20]

CO was calculated using the indicator-dilution principle and the arterial input functions. In addition, LV mass was obtained from the dynamic data set using parametric images and contour detection, as described in detail elsewhere.[21]

## Echocardiography

We used a commercially available ultrasound system (Vivid E95; GE Healthcare, Horten, Norway) with a 3.5-MHz-phased array transducer (M5S).

At rest, CA patients and controls underwent a comprehensive echocardiographic assessment according to current guidelines.[23]

Only CA patients were subjected to exercise testing. At each stage of exercise, we assessed two-dimensional cine loops and tissue Doppler images from all 3 apical views of the LV along with pulsed wave Doppler of the mitral inflow and the left ventricular outflow tract (LVOT). Left ventricular ejection fraction (LVEF) was calculated by Simpson's biplane method of disks. Peak systolic mitral annular velocities (S′) were estimated from the tissue Doppler velocity images as an average of septal, lateral, anterior, and posterior velocities. The magnitude of LVGLS[24] was obtained from frame-by-frame tracking of speckle patterns throughout the left-sided myocardium in standard two-dimensional cine loops with a frame rate >55 frames/s. LVGLS was calculated at the time in systole when the value peaked, using a 17-myocardial segment model.[25] In this manuscript, strain and changes in strain are reported in absolute terms.

We obtained three-dimensional LV mass by sampling 6 heartbeats during breath-hold, aiming at a frame rate >25 frames/s using a 4V-D transducer. We measured both diastolic and systolic LV mass. An average of the 2 was used to calculate three-dimensional LV mass. Three-dimensional LV mass has been validated in several studies, which show that LV mass measured by three-dimensional echocardiography is similar to that measured by magnetic resonance imaging.[26–29]

Data were analyzed offline using dedicated software (EchoPAC PC SW-Only, 201, GE-Healthcare, Milwaukee, WI, USA and TomTec 4D RV-function, Munich, Germany).

## Exercise Protocol

All patients with CA performed a multistage symptom-limited, semi-supine bicycle exercise test using the Echo Cardiac Stress Table (Lode B.V., Netherlands). Workload started at 0 W and was increased by 25 W every 3 minutes in New York Heart Association (NYHA) class ≤II patients and by 10 W in NYHA class ≥III patients. Patients were explicitly encouraged to maintain a fixed pedaling speed of 60 rounds per minute and to exercise until exhaustion (Borg >18).[30] During exercise, external oxygen consumption ($VO_2$) was measured by breath-by-breath analysis of expired gas. The ratio between cardiac output (CO) increase by thermodilution (peak CO−rest CO) and $VO_2$ increase (peak $VO_2$−rest $VO_2$) was used as cardiac response marker to metabolic needs.[31]

## Right Heart Catheterization

Right heart catheterization was performed in CA patients with a standard 7.5-F triple-lumen Swan-Ganz thermistor using a balloon-tipped catheter (Edwards Lifesciences, Irvine, CA). The catheter was introduced into the right jugular vein using an ultrasound-guided technique and advanced pressure waveforms and fluoroscopy guided into the pulmonary artery. A comprehensive, direct, and indirect assessment of hemodynamic parameters was performed at rest and during exercise as described in a previous publication.[17]

## Myocardial Work and Efficiency

Average heart rate and mean arterial blood pressure measurements obtained during PET examination were used to calculate MEE.[9]

$$\mathrm{MEE} = \frac{\mathrm{EW} \times 1.33 \times 10^{-4}}{\mathrm{LV\ mass} \times \mathrm{MVO_2} \times 20} \times 100$$

EW (mm Hg/mL per minute) was calculated as the product of PET derived stroke volume, heart rate, and mean arterial blood pressure. In this equation, the numerator represents EW (in joules) and the denominator represents the energetic value of the total $O_2$ amount consumed by the left ventricle. The constants $1.33 \times 10^{-3}$ and 20 were used for conversion of cardiac minute work and $MVO_2$ to joules.

In a similar manner, the average heart rate and mean arterial blood pressure measurements obtained during resting and exercise echocardiography was used to calculate echocardiographic MWE as:

$$\mathrm{MWE} = \frac{\mathrm{EW}}{\mathrm{3D\ LV\ mass}}$$

EW by echocardiography was calculated as the product of LVOT area, velocity time integral, heart rate, and mean arterial blood pressure.

## Statistical Analysis

Normally distributed data are presented as mean±SD; non-normally distributed data are presented as median and interquartile range. Categorical data are presented as numbers with percentages. Histograms and Q-Q plots were used to check continuous values for normality. Between-group differences were assessed using the *t* test for normally distributed data, the Mann–Whitney *U* test for non-normally distributed data, and the Chi-squared test for dichotomized data. A linear regression model was used to compare continuous variables. We calculated Pearson's coefficient of correlation in normally distributed data and Spearman's coefficient of correlation in non-normally distributed data. All tests were 2-sided, and a $P<0.05$ was considered statistically significant. Analyses were performed using STATA (STATA/IC 13, StataCorp LP, College Station, TX).

# Results

## Patient Characteristics

Table 1 presents the demographics of patients and control subjects. We found no significant difference between age and sex comparing CA patients and controls. As depicted, the majority of CA patients were symptomatic with high use of diuretics. However, only few CA patients received angiotensin-converting-enzyme/ATII (ACE/ATII) inhibitors, beta-blockers, and aldosterone inhibitors. NT-ProBNP (N-terminal pro-B-type natriuretic peptide) was significantly higher in CA patients than controls.

## Transthoracic Echocardiography

The CA patients had significantly reduced LV systolic function compared with controls at rest (LV-EF 54±13% versus 63±4%, $P<0.05$; LV-S′ 4.4±1.8 cm/s versus 6.4±1.2 cm/s, $P<0.001$; LV-GLS 12±4% versus 19±2%, $P<0.0001$). The regional strain analysis reveal apical sparring pattern in the CA patients with a mean difference between apical segments and basal segments of 9.7±4.2%. The basal segments showed no deformation increase during exercise whereas strain in the apical segments was more pronounced at peak exercise. The mean increase in apical to basal strain difference with exercise was 3.2±5.2%. We found a significant relationship between the exercise induced apical to basal strain difference and symptom burden by New York Heart Association (NYHA) functional class ($r^2=0.23$, $P<0.05$) and peak exercise metabolic equivalent of tasks ($r^2=0.19$, $P<0.05$) and peak exercise $VO_2$ ($r^2=0.28$, $P<0.05$).

The CA patients had a more restrictive LV filling pattern than controls (E/A ratio: 1.7 [1.2–3.2] versus 1.1 [1.0–1.6], $P<0.05$; E-deceleration time 168±52 ms versus 210±49 ms, $P<0.05$; E/e′ 18 [12–25] versus 8 [7–9], $P<0.0001$).

Echocardiographic parameters in CA patients at rest and at peak exercise are depicted in Table 2.

**Table 1.** Patient Characteristics

| | Controls (n=10) | All CA Patients (n=25) | *P* Value |
|---|---|---|---|
| Male, % | 30 | 80 | <0.01 |
| BMI, kg/m$^2$ | 26±4 | 25±3 | 0.30 |
| BSA, m$^2$ | 2.0±0.2 | 1.9±0.2 | 0.45 |
| Age, y | 64 [62–66] | 69 [55–78] | 0.27 |
| NYHA functional class >I, % | 0 | 68 | <0.001 |
| Hypertension, % | 0 | 24 | 0.09 |
| Medication | | | |
| Statins, % | 0 | 20 | 0.13 |
| ACE/Angiotensin II inhibitor, % | 0 | 24 | 0.09 |
| Beta blockers, % | 0 | 28 | 0.06 |
| Furosemide or bumetanide, % | 0 | 64 | 0.001 |
| Thiazide, % | 0 | 8 | 0.36 |
| Spironolactone, % | 0 | 16 | 0.18 |
| Biochemistry | | | |
| Creatinine, μmol/L | 84 [72–92] | 106 [83–134] | <0.05 |
| Hemoglobin, mmol/L | 8.7±0.6 | 8.4±1.0 | 0.33 |
| NT-ProBNP, ng/L | 33 [27–74] | 1962 [674–4268] | <0.0001 |

Data are presented as absolute number and present or mean±SD or median and interquartile range. ACE indicates acetylcholinesterase; BMI, body mass index; BSA, body surface area; NT-ProBNP, N-terminal pro-B-type natriuretic peptide; NYHA, New York Heart Association.

## Invasive Hemodynamics

Invasive hemodynamic parameters at rest and at peak exercise are shown in Table 2. During resting conditions, mean LV and right ventricular filling pressure were only slightly elevated and cardiac index (CI) was within normal range in the majority of patients. However, during exercise, a profound increase in LV and right ventricular filling pressure were noted with only a small increase in CI despite adequate increase in heart rate.

## $MVO_2$ and External Efficiency

Table 3 shows the results from $^{11}$C-acetate PET in CA patients and controls whereas Table 4 shows the relationship between MEE and myocardial function in CA patients. Total $MVO_2$ (mL/min) was significantly higher in CA patients than controls. Furthermore, patients with CA had significantly lower EW than controls. Subsequently, MEE was severely reduced in CA patients compared with controls. MEE decreased with advanced symptom burden by NYHA functional class (Figure 1). We found a good relationship between MEE and LVGLS and between MEE and echocardiographic derived MWE (Figures 2 and 3). Likewise, we found a good relationship between MEE and invasively derived pulmonary arterial compliance and CI (Figures 2 and 4). These relationships were seen both at rest and during exercise. In contrast, MEE poorly correlated with invasive filling pressures and non-invasive LV filling pattern by echocardiography both at resting and during exercise (Figure 4 and Table 4). We found no difference in MEE between AL and ATTR CA patients (14.3±6.4% versus 12.4±4.6%, $P=0.41$). Likewise, we found no difference in total $MVO_2$ between AL and ATTR CA patients (17±6 versus 19±6, $P=0.44$).

**Table 2.** Myocardial Function by Right Heart Catheterization and by Echocardiography in Cardiac Amyloidosis Patients

| | Resting Conditions | Peak Exercise | *P* Value |
|---|---|---|---|
| Hemodynamics | | | |
| MAP, mm Hg | 90±10 | 104±27 | <0.05 |
| HR, beats/min | 76±17 | 123±27 | <0.0001 |
| CI, L/min per $m^2$ | 2.3±0.6 | 4.4±2.1 | <0.0001 |
| $VO_2$, mL/min per kg | 301±89 | 1156±496 | <0.0001 |
| mRAP, mm Hg | 6.8±4.4 | 16±9 | <0.0001 |
| mPAP, mm Hg | 25±9 | 46±11 | <0.0001 |
| mPCWP, mm Hg | 15±7 | 31±8 | <0.0001 |
| PAC, mL/mm Hg | 3.6±2.3 | 2.6±1.7 | <0.01 |
| Echocardiography | | | |
| IVS, mm | 15.8±5.0 | | |
| PWT, mm | 13.8±3.6 | | |
| 3D LV mass, g/$m^2$ | 129±33 | | |
| 2D LVEF Simpson Biplane, % | 54±13 | 57±14 | 0.10 |
| LVGLS, % | 12±4 | 13±6 | 0.12 |
| Strain apical segments, % | 17±5 | 21±8 | <0.01 |
| Strain basal segments, % | 7.5±5.3 | 7.7±6.4 | 0.74 |
| A-B strain diff, % | 9.7±4.2 | 12.9±4.7 | <0.01 |
| MWE, mm Hg L/min per g | 1.9±1.0 | 4.4±3.6 | <0.001 |
| E/A (ratio) | 2.2±1.4 | 2.4±1.2 | 0.97 |
| E/e′ (ratio) | 22±13 | 22±14 | 0.76 |
| LA volume, mL/$m^2$ | 42±19 | | |
| RA volume, mL/$m^2$ | 34±22 | | |
| TAPSE, cm | 1.8±0.7 | | |
| RVS′, cm/s | 8.9±2.4 | | |

2D indicates two-dimensional; 3D, three-dimensional; A-B, apical to basal; CI, cardiac index; HR, heart rate; IVS, interventricular septal thickness; LA, left atrium; LVEF, left ventricular ejection fraction; LVGLS, left ventricular global longitudinal strain; MAP, mean arterial blood pressure; mPAP, mean pulmonary artery pressure; mPCWP, mean pulmonary capillary wedge pressure; mRAP, mean right atrial pressure; MWE, myocardial work efficiency; PAC, pulmonary arterial compliance; PWT, posterior wall thickness; RA, right atrium; RVS', peak systolic velocity of tricuspid annulus; TAPSE, tricuspid annular plane systolic excursion; $VO_2$, external oxygen consumption.

## Myocardial Blood Flow

MBF tended to be lower in CA patients than controls (Table 3). We found a significant relationship between MBF and systolic performance (LVGLS: $r^2$=0.45, $P$<0.0001 CI: $r^2$=0.31, $P$<0.001) and between MBF and LV mass ($r^2$=0.25, $P$<0.05). In contrast, MBF did not correlate with LV or right ventricular filling pressure (PCWP: $r^2$=0.03, $P$=0.44; right atrial pressure: $r^2$=0.04, $P$=0.37).

In CA patients $MVO_2$ (per gram tissue) correlated significantly with MBF ($r^2$=0.42, $P$<0.0001), whereas the total $MVO_2$ did not correlate with MBF ($r^2$=0.01, $P$=0.61). Furthermore, a strong relationship was seen between MEE and MBF in the CA patients ($r^2$=0.44, $P$<0.0001).

## Discussion

This is the first study to evaluate myocardial oxidative metabolism, myocardial perfusion, and the coupling to invasive and non-invasive myocardial contractile work parameters in CA patients. The 4 main findings were (1) that CA patients display substantially increased total $MVO_2$ and reduced MEE independent of etiology; (2) MEE correlates significantly with MBF; (3) the observed reduction in MEE is associated with decreasing systolic myocardial performance and with increasing symptom burden; and (4) MEE did not correlate with invasive or non-invasive parameters of LV filling pressure.

Myocardial function is highly dependent on myocardial oxidative metabolism and the coupling to contractile work. In CA, the oxidative metabolism may be affected by both structural damage (both AL and transthyretin-related [TTR]) and proteotoxicity (AL). In the latter, circulating cardiotoxic light chains are suggested to produce cellular damage through various pathways ie, increase in cellular reactive oxygen species and up-regulation of heme oxygenase both leading to impaired contractility and relaxation.[4] MEE integrates contractile function, loading conditions and metabolic

**Table 3.** $^{11}$C-Acetate Positron Emission Tomography

| | Controls (n=10) | All CA Patients (n=25) | *P* Value |
|---|---|---|---|
| MEE, % | 24±5 | 13±5 | <0.0001 |
| EW, mm Hg× mL/min×$10^3$ | 446±103 | 346±142 | 0.05 |
| Total $MVO_2$, mL/min | 13±3 | 18±6 | <0.01 |
| $MVO_2$, mL/min per g | 0.10±0.02 | 0.09±0.02 | 0.22 |
| MBF, mL/min per g | 0.67±0.11 | 0.59±0.18 | 0.11 |
| Total work, J | 59±14 | 46±19 | 0.05 |
| HR, beats/min | 62±8 | 73±12 | <0.01 |
| MAP, mm Hg | 94±7 | 78±11 | <0.001 |
| LV mass index, g/$m^2$ | 63±12 | 103±29 | <0.001 |
| CI, L/min per $m^2$ | 2.4±0.6 | 2.2±0.6 | 0.46 |
| SVI, mL/$m^2$ | 39±7 | 31±9 | <0.05 |

Data are presented as mean±SD or median and interquartile range. CI indicates cardiac index; EW, external stroke work; HR, heart rate; LV, left ventricular; MAP, mean arterial blood pressure; MBF, myocardial blood flow; MEE, myocardial external efficiency; $MVO_2$, myocardial oxygen consumption; SVI, stroke volume index.

**Table 4.** Univariate and LV Mass Adjusted Correlations Between PET-Derived Myocardial External Efficiency and Myocardial Function in CA Patients

| | Unadjusted | | LV Mass Adjusted | |
|---|---|---|---|---|
| | $R^2$ | *P* Value | $R^2$ | *P* Value |
| Echocardiography | | | | |
| E/e′ | 0.14 | 0.07 | … | … |
| $MWE_{rest}$ | 0.51 | <0.0001 | 0.57 | <0.0001 |
| $MWE_{peak}$ | 0.48 | <0.0001 | 0.50 | <0.01 |
| $LVGLS_{rest}$ | 0.61 | <0.0001 | 0.61 | <0.0001 |
| $LVGLS_{peak}$ | 0.60 | <0.0001 | 0.60 | <0.0001 |
| ΔA-B strain difference | 0.27 | <0.01 | 0.40 | <0.05 |
| 3D LV mass | 0.39 | <0.01 | … | … |
| Invasive hemodynamics | | | | |
| $\Delta CO/\Delta VO_2$ | 0.21 | <0.05 | 0.35 | <0.05 |
| $CI_{rest}$ | 0.36 | <0.01 | 0.46 | <0.01 |
| $CI_{peak}$ | 0.52 | <0.0001 | 0.55 | <0.01 |
| $SV_{res}$ | 0.37 | <0.01 | 0.53 | <0.01 |
| $SV_{peak}$ | 0.44 | <0.01 | 0.63 | <0.0001 |
| $VO_{2peak}$ | 0.31 | <0.01 | 0.42 | <0.01 |
| $PCWP_{rest}$ | 0.11 | 0.13 | … | … |
| $PCWP_{peak}$ | 0.04 | 0.40 | … | … |
| $PAC_{rest}$ | 0.43 | <0.01 | 0.46 | <0.01 |
| $PAC_{peak}$ | 0.43 | <0.01 | 0.45 | <0.01 |
| $RAP_{rest}$ | 0.11 | 0.14 | … | … |
| $RAP_{peak}$ | 0.13 | 0.11 | … | … |
| PET-derived parameters | | | | |
| MBF | 0.44 | <0.0001 | 0.46 | <0.01 |
| Total work | 0.44 | <0.0001 | 0.76 | <0.0001 |
| Total $MVO_2$ | 0.14 | 0.07 | … | … |

3D indicates three-dimensional; A-B, apical to basal; CA, cardiac amyloidosis; CI, cardiac index; CO, cardiac output; LV, left ventricular; LVGLS, left ventricular global longitudinal strain; MBF, myocardial blood flow; $MVO_2$, myocardial oxygen consumption; MWE, myocardial work efficiency; PAC, pulmonary arterial compliance; PCWP, pulmonary capillary wedge pressure; PET, positron emission tomography; RAP, right atrial pressure; SV, stroke volume; $VO_2$, external oxygen consumption.

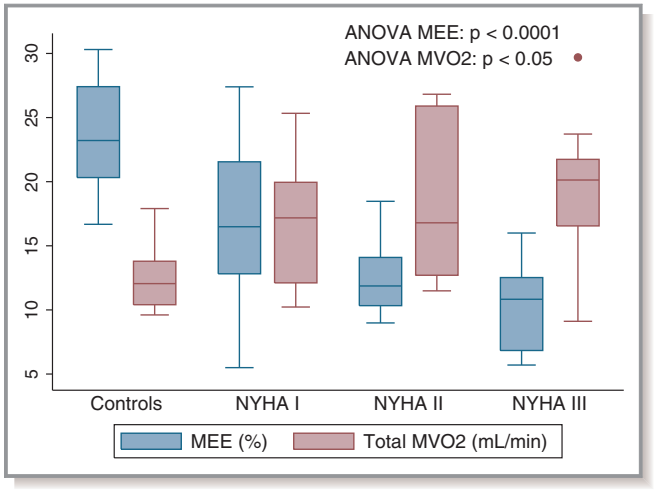


**Figure 1.** Box plots showing myocardial external efficiency (MEE) and myocardial oxygen consumption ($MVO_2$) in controls and CA patients stratified into New York Heart Association (NYHA) groups.

requirements and is potentially a robust marker of cardiac function irrespective of underlying pathology. To our knowledge, the current study is the first to investigate MEE in CA patients.

The myocardial thickness in CA is mediated both by interstitial amyloid deposits and by myocardial hypertrophy. Thus, the oxidative metabolism per gram heart tissue does not reflect the overall metabolic state of the myocytes. In contrast, the increase in total myocardial oxygen consumption during resting conditions clearly indicates that the myocyte mitochondrial oxidative phosphorylation rate is abnormal in the CA population. Interestingly, it was demonstrated that total $MVO_2$ and MEE was abnormal even in CA patients in NYHA class I. This indicates that myocardial oxidative metabolism may deteriorate before the development of symptoms. Thus, the inefficient myocardial energy exploitation and mitochondrial uncoupling may play a central role in the transition to symptomatic heart failure in CA patients as also suggested in heart failure patients with different etiologies than CA.[6–8]

Traditionally, the amyloid-induced restrictive cardiomyopathy is characterized by abnormal LV filling with reduced cardiac output despite preserved LVEF.[5] However, our recent studies[16,17] suggests, that exercise capacity and symptoms in CA patients are strongly associated with the myocardial perfusion reserve and systolic myocardial capacity in terms of peak exercise CI and LVGLS. The latter has emerged as a novel non-invasive parameter to determine the functional CA burden and possesses great prognostic value in these patients.[32–40] In the present study, we demonstrate a good relationship between LVGLS and MBF, between LVGLS and MEE, and between MEE and MBF. It is noteworthy that both resting LVGLS, peak exercise LVGLS and the exercise induced apical to basal strain difference correlated with MEE. Apical sparing of longitudinal strain is a well-known finding in CA patients but the underlying pathophysiology is not fully elucidated. Our results suggest that the apical myocardial contractile reserve is of significant importance to preserve overall MEE. Perfusion abnormalities may result in an energy-starved myocardium. Because of the endocardial location of the longitudinally orientated fibers, these are the myocardial fibers most vulnerable to reduced perfusion. This may explain the good correlation between LVGLS and MBF. Similar findings have been demonstrated in a small study by Dorbala

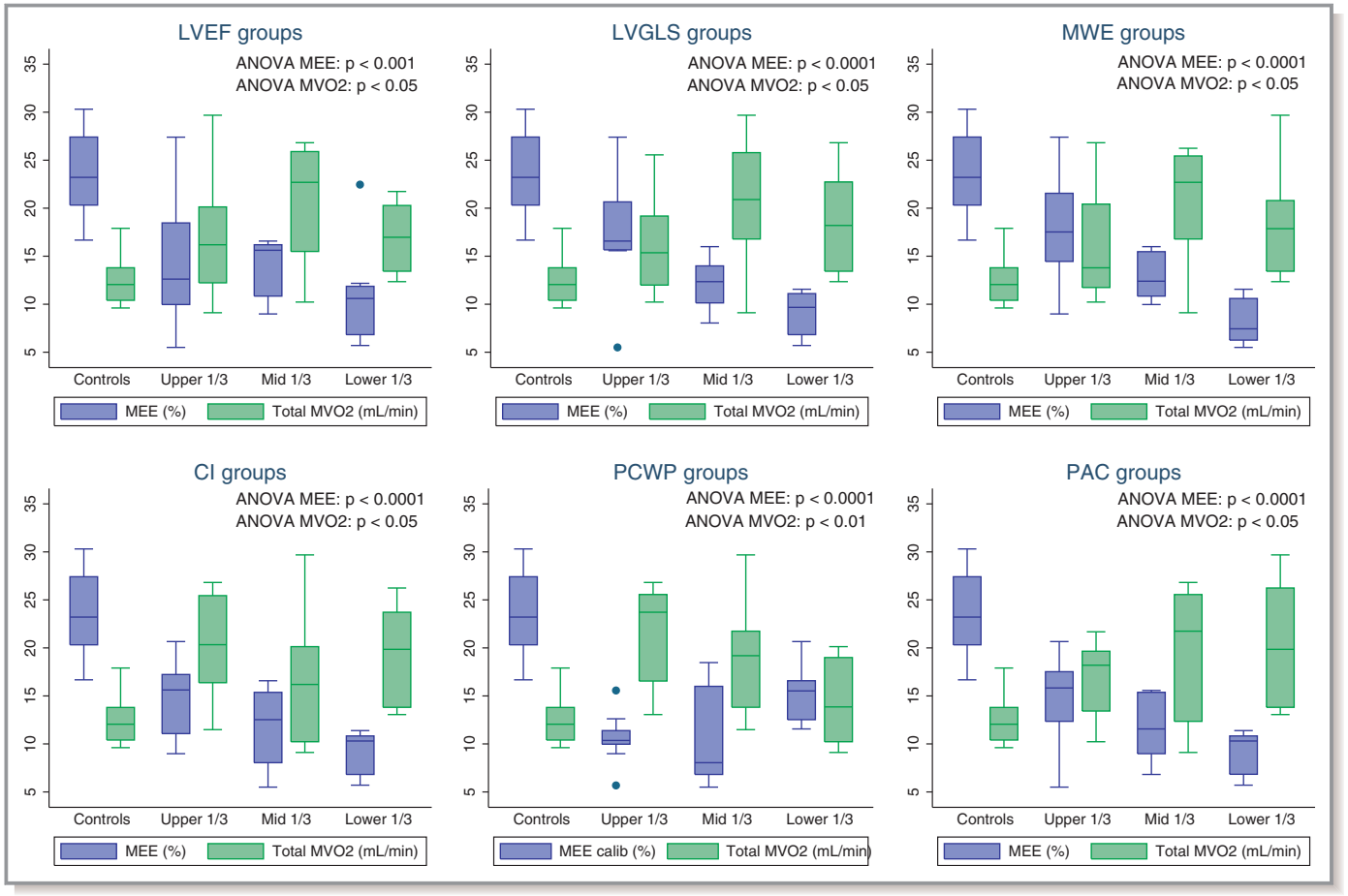


**Figure 2.** Box plots showing myocardial external efficiency (MEE) and myocardial oxygen consumption ($MVO_2$) in controls and CA patients stratified into tertiles of resting left ventricular ejection fraction (LVEF), left ventricular global longitudinal strain (LVGLS), myocardial work efficiency (MWE), cardiac index (CI), pulmonary capillary wedge pressure (PCWP), and pulmonary arterial compliance (PAC).

et al, who evaluated the myocardial perfusion by using $^{13}$N-ammonia PET.[41] Dorbala et al found a profound coronary microcirculatory dysfunction in CA patients compared with left ventricular hypertrophy subjects with non-amyloid etiology. The abnormal myocardial perfusion was also demonstrated to be significantly associated with longitudinal myocardial deformation by two-dimensional echocardiography. We speculate that regional myocardial perfusion abnormalities may be associated with regional myocardial deformation differences and subsequently the development of relative apical sparing of longitudinal strain. However, in addition to the perfusion abnormalities, the amyloid deposits might lead to inefficient energy exploitation and mitochondrial uncoupling subsequently resulting in decreased myocardial contractility. Therefore, the increased oxygen consumption noted in CA patients may be a compensatory mechanism to maintain adequate cardiac output despite perfusion abnormalities and inefficient energy exploitation. Cardiac output will usually decrease when either preload or myocardial contractility is reduced or when the afterload increases. Yet, both left and right side resting filling pressures in CA patients were slightly higher than normal range.[42] Furthermore, the CA patients had lower blood pressure than controls. Therefore, the reduced cardiac output demonstrated in CA patients seems most likely to be induced by an inherently reduced contractility. Potentially, the reduced MEE may be an important component in the poor myocardial contractility seen in CA patients.

Previous studies have demonstrated that the prognosis in AL patients is poorer as compared with ATTR CA patients,[4] even though the myocardial thickness is more pronounced in ATTR patients indicating a higher degree of amyloid deposition. Therefore, it has been speculated that AL fibers may induce a greater proteotoxicity than ATTR fibers.[4] In the present study, we found no statistically or clinically significant differences in MEE and total $MVO_2$ between AL and ATTR CA patients. Therefore, the present study does not support the hypothesis that poor prognosis in AL patients is induced by abnormal mitochondrial function. However, the differences in myocardial performance and oxidative metabolism between

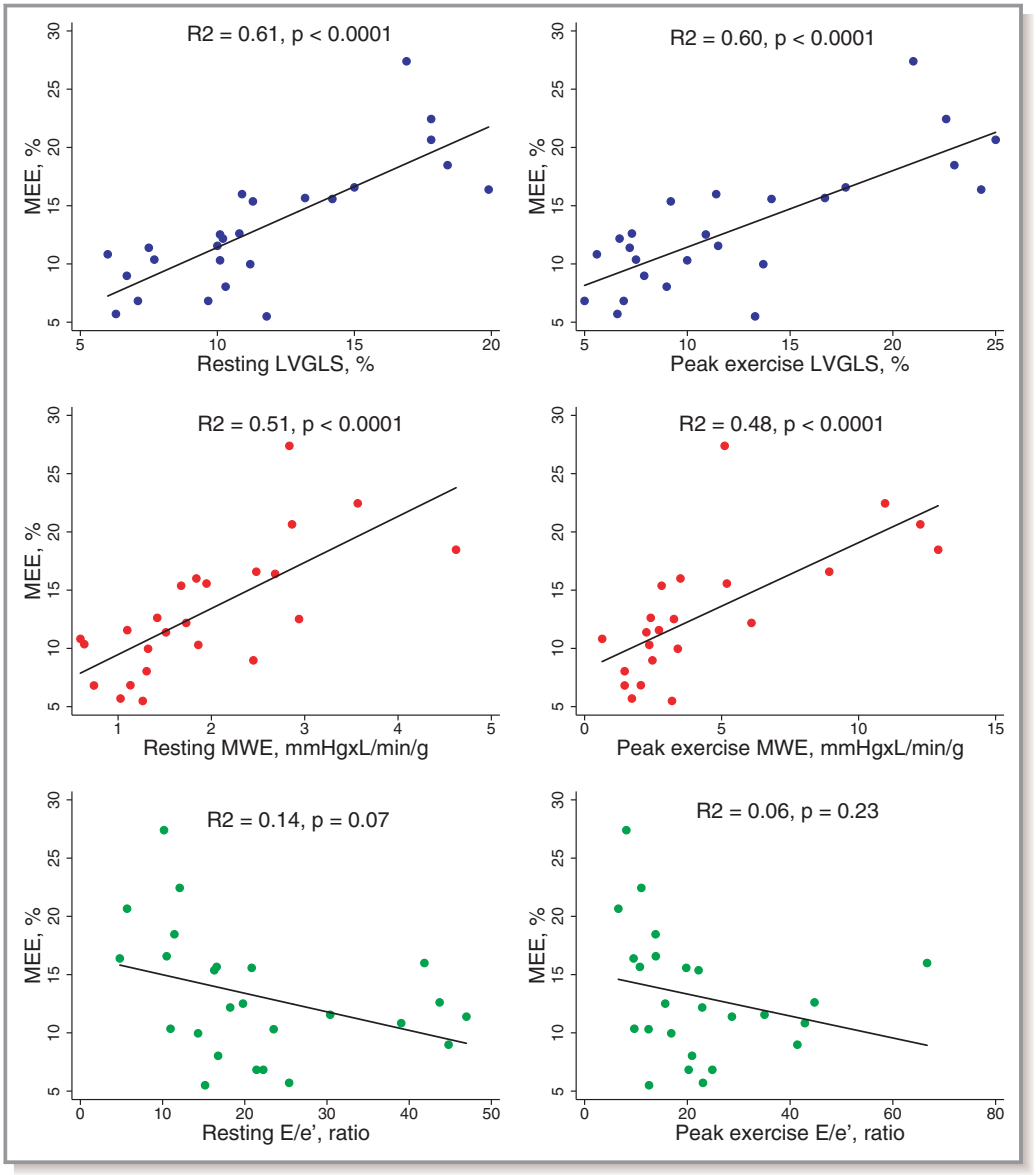


**Figure 3.** Scatter plots with regression lines showing the relationship between myocardial external efficiency (MEE) and left ventricular global longitudinal strain (LVGLS), myocardial work efficiency (MWE), and E/e′ ratio in cardiac amyloidosis patients at rest and at peak exercise.

ATTR and AL subjects should be investigated in a larger study.

In the present study, we assessed MEE solely by $^{11}$C-acetate PET. This approach has been validated against the combination of $^{11}$C-acetate PET and cardiac magnetic resonance (MR), which until today has been considered the gold-standard method for non-invasive quantification of MEE.[43] A strong association has been demonstrated between LV mass and stroke volume by $^{11}$C-acetate PET and cardiac MR.[21,44] The simultaneous acquisition of both EW and total $MVO_2$ makes MEE less affected by changes in loading conditions. $MVO_2$ per gram myocardial tissue is a rather stable parameter in patients with myocardial hypertrophy attributable to aortic valve stenosis.[10] With the assumption that $MVO_2$ per gram myocardial tissue is a stable parameter in CA patients, myocardial efficiency can be calculated by MWE, which reflects the myocardial ability to conduct work. The present study demonstrated, that $MVO_2$ per gram myocardial tissue was indeed similar between healthy controls and CA patients. Therefore, MWE assessment may prove beneficial as a simple and more accessible alternative to MEE assessment by PET; moreover, it can be performed bedside, rapidly, and without radiation.

Routine surveillance of CA patients is of great importance to optimize loading conditions and detect deterioration of myocardial function. Even though $^{11}$C-acetate PET may harbor

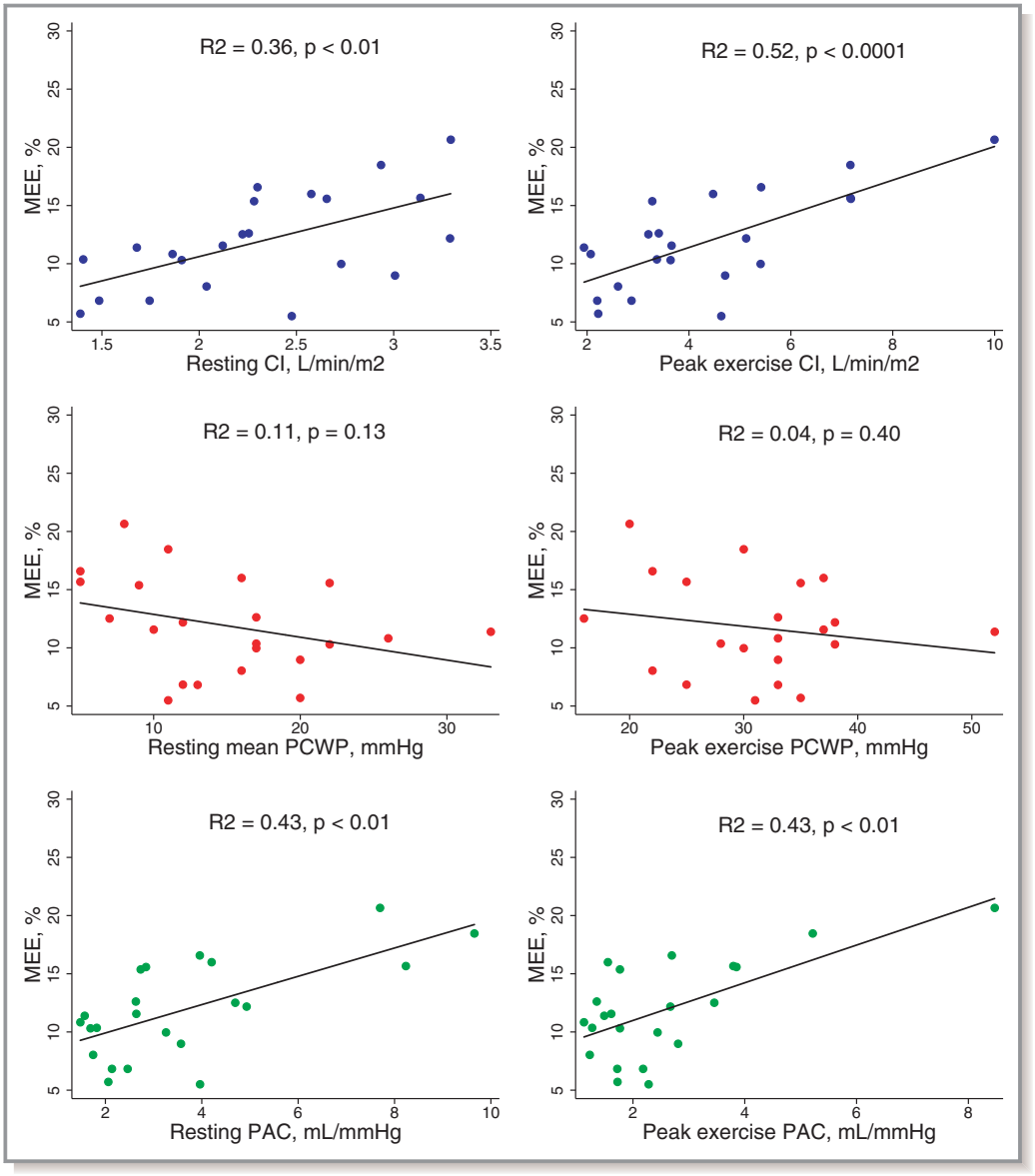


**Figure 4.** Scatter plots with regression lines showing the relation between myocardial external efficiency (MEE) and cardiac index (CI), pulmonary capillary wedge pressure, and pulmonary arterial compliance (PAC) in cardiac amyloidosis patients at rest and at peak exercise.

great value in the assessment of MEE and MBF, the technique is currently only available in a few highly specialized centers. In contrast, the good relationship between echocardiographic LVGLS and PET determined MEE and MBF emphasizes the importance of routine LVGLS assessment in CA patients.

## Conclusion

The total oxidative myocardial metabolism is significantly increased without any correlation to myocardial perfusion or external efficiency in CA patients. Myocardial external efficiency is significantly reduced in CA patients and correlated significantly with echocardiographic-derived systolic parameters such as MWE and LVGLS that might be used as surrogate MEE markers.

## Limitations

This study is a single-centered experience with a relatively limited number of patients. Therefore, we were unable to simultaneously control for several variables in the study and to define the causal relationship of the described associations. ATTRwt were older and more likely to be men than AL patients and controls. Age and sex may influence both myocardial perfusion, myocardial oxidative metabolism, and

LV deformation capacity. In our MEE and MWE calculations, we assumed that all LV mass is myocardial mass. Yet, LV mass in CA patients consists of both myocardial and non-myocardial tissue (ie amyloid deposits). $MVO_2$ is based on washout rate and consequently represents $MVO_2$ in oxygen-consuming tissue only. Therefore, $MVO_2$ could be myocardial-only-$MVO_2$ while LV mass is both myocardial and amyloid mass. This could be an explanation for the similar $MVO_2$/g but difference in total $MVO_2$. The calculated MEE and MWE therefore does not reflect the efficiency of the isolated myocytes but rather the efficiency of the total myocardium.

## Acknowledgments

We would like to extend our gratitude to the nurses at the outpatient clinic of the Department of Cardiology, Aarhus University Hospital, Skejby, Denmark for their invaluable assistance during stress testing.

## Disclosures

None.

## References

1. Quarta CC, Kruger JL, Falk RH. Cardiac amyloidosis. *Circulation*. 2012;126:e178–e182.
2. Falk RH. Cardiac amyloidosis: a treatable disease, often overlooked. *Circulation*. 2011;124:1079–1085.
3. Falk RH, Comenzo RL, Skinner M. The systemic amyloidoses. *N Engl J Med*. 1997;337:898–909.
4. Falk RH, Alexander KM, Liao R, Dorbala S. AL (light-chain) cardiac amyloidosis: a review of diagnosis and therapy. *J Am Coll Cardiol*. 2016;68:1323–1341.
5. Gertz MA, Benson MD, Dyck PJ, Grogan M, Coelho T, Cruz M, Berk JL, Plante-Bordeneuve V, Schmidt HHJ, Merlini G. Diagnosis, prognosis, and therapy of transthyretin amyloidosis. *J Am Coll Cardiol*. 2015;66:2451–2466.
6. Neubauer S. The failing heart—an engine out of fuel. *N Engl J Med*. 2007;356:1140–1151.
7. Kim IS, Izawa H, Sobue T, Ishihara H, Somura F, Nishizawa T, Nagata K, Iwase M, Yokota M. Prognostic value of mechanical efficiency in ambulatory patients with idiopathic dilated cardiomyopathy in sinus rhythm. *J Am Coll Cardiol*. 2002;39:1264–1268.
8. Bing RJ, Hammond MM. The measurement of coronary blood flow, oxygen consumption, and efficiency of the left ventricle in man. *Am Heart J*. 1949;38:1–24.
9. Knaapen P, Germans T, Knuuti J, Paulus WJ, Dijkmans PA, Allaart CP, Lammertsma AA, Visser FC. Myocardial energetics and efficiency: current status of the noninvasive approach. *Circulation*. 2007;115:918–927.
10. Hansson NH, Sorensen J, Harms HJ, Kim WY, Nielsen R, Tolbod LP, Frokiaer J, Bouchelouche K, Dodt KK, Sihm I, Poulsen SH, Wiggers H. Myocardial oxygen consumption and efficiency in aortic valve stenosis patients with and without heart failure. *J Am Heart Assoc*. 2017;6:e004810. DOI: 10.1161/JAHA.116.004810.
11. Suga H. Ventricular energetics. *Physiol Rev*. 1990;70:247–277.
12. Gillmore JD, Maurer MS, Falk RH, Merlini G, Damy T, Dispenzieri A, Wechalekar AD, Berk JL, Quarta CC, Grogan M, Lachmann HJ, Bokhari S, Castano A, Dorbala S, Johnson GB, Glaudemans AW, Rezk T, Fontana M, Palladini G, Milani P, Guidalotti PL, Flatman K, Lane T, Vonberg FW, Whelan CJ, Moon JC, Ruberg FL, Miller EJ, Hutt DF, Hazenberg BP, Rapezzi C, Hawkins PN. Nonbiopsy diagnosis of cardiac transthyretin amyloidosis. *Circulation*. 2016;133:2404–2412.
13. Lee SP, Lee ES, Choi H, Im HJ, Koh Y, Lee MH, Kwon JH, Paeng JC, Kim HK, Cheon GJ, Kim YJ, Kim I, Yoon SS, Seo JW, Sohn DW. $^{11}$C-Pittsburgh B PET imaging in cardiac amyloidosis. *JACC Cardiovasc Imaging*. 2015;8:50–59.
14. Pilebro B, Arvidsson S, Lindqvist P, Sundstrom T, Westermark P, Antoni G, Suhr O, Sorensen J. Positron emission tomography (PET) utilizing Pittsburgh compound B (PIB) for detection of amyloid heart deposits in hereditary transthyretin amyloidosis (ATTR). *J Nucl Cardiol*. 2018;25:240–248.
15. Antoni G, Lubberink M, Estrada S, Axelsson J, Carlson K, Lindsjo L, Kero T, Langstrom B, Granstam SO, Rosengren S, Vedin O, Wassberg C, Wikstrom G, Westermark P, Sorensen J. In vivo visualization of amyloid deposits in the heart with $^{11}$C-PIB and PET. *J Nucl Med*. 2013;54:213–220.
16. Clemmensen TS, Eiskjaer H, Molgaard H, Larsen AH, Soerensen J, Andersen NF, Tolbod LP, Harms HJ, Poulsen SH. Abnormal coronary flow velocity reserve and decreased myocardial contractile reserve are main factors in relation to physical exercise capacity in cardiac amyloidosis. *J Am Soc Echocardiogr*. 2018;31:71–78.
17. Clemmensen TS, Molgaard H, Sorensen J, Eiskjaer H, Andersen NF, Mellemkjaer S, Andersen MJ, Tolbod LP, Harms HJ, Poulsen SH. Inotropic myocardial reserve deficiency is the predominant feature of exercise haemodynamics in cardiac amyloidosis. *Eur J Heart Fail*. 2017;19:1457–1465.
18. Hansson NH, Tolbod L, Harms J, Wiggers H, Kim WY, Hansen E, Zaremba T, Frokiaer J, Jakobsen S, Sorensen J. Evaluation of ECG-gated [(11)C]acetate PET for measuring left ventricular volumes, mass, and myocardial external efficiency. *J Nucl Cardiol*. 2016;23:670–679.
19. Harms HJ, Knaapen P, de Haan S, Halbmeijer R, Lammertsma AA, Lubberink M. Automatic generation of absolute myocardial blood flow images using [$^{15}$O]$H_2O$ and a clinical PET/CT scanner. *Eur J Nucl Med Mol Imaging*. 2011;38:930–939.
20. Sun KT, Yeatman LA, Buxton DB, Chen K, Johnson JA, Huang SC, Kofoed KF, Weismueller S, Czernin J, Phelps ME, Schelbert HR. Simultaneous measurement of myocardial oxygen consumption and blood flow using [1-carbon-11] acetate. *J Nucl Med*. 1998;39:272–280.
21. Harms HJ, Stubkjaer Hansson NH, Tolbod LP, Kim WY, Jakobsen S, Bouchelouche K, Wiggers H, Frokiaer J, Sorensen J. Automatic extraction of myocardial mass and volume using parametric images from dynamic nongated PET. *J Nucl Med*. 2016;57:1382–1387.
22. van den Hoff J, Burchert W, Borner AR, Fricke H, Kuhnel G, Meyer GJ, Otto D, Weckesser E, Wolpers HG, Knapp WH. 1-(11)C]Acetate as a quantitative perfusion tracer in myocardial PET. *J Nucl Med*. 2001;42:1174–1182.
23. Lang RM, Badano LP, Mor-Avi V, Afilalo J, Armstrong A, Ernande L, Flachskampf FA, Foster E, Goldstein SA, Kuznetsova T, Lancellotti P, Muraru D, Picard MH, Rietzschel ER, Rudski L, Spencer KT, Tsang W, Voigt JU. Recommendations for cardiac chamber quantification by echocardiography in adults: an update from the American Society of Echocardiography and the European Association of Cardiovascular Imaging. *J Am Soc Echocardiogr*. 2015;28:1–39.e14.
24. Reisner SA, Lysyansky P, Agmon Y, Mutlak D, Lessick J, Friedman Z. Global longitudinal strain: a novel index of left ventricular systolic function. *J Am Soc Echocardiogr*. 2004;17:630–633.
25. Cerqueira MD, Weissman NJ, Dilsizian V, Jacobs AK, Kaul S, Laskey WK, Pennell DJ, Rumberger JA, Ryan T, Verani MS; American Heart Association Writing Group on Myocardial Segmentation and Registration for Cardiac Imaging. Standardized myocardial segmentation and nomenclature for tomographic imaging of the heart. A statement for healthcare professionals from the Cardiac Imaging Committee of the Council on Clinical Cardiology of the American Heart Association. *Circulation*. 2002;105:539–542.
26. Qin JX, Jones M, Travaglini A, Song JM, Li J, White RD, Tsujino H, Greenberg NL, Zetts AD, Panza JA, Thomas JD, Shiota T. The accuracy of left ventricular mass determined by real-time three-dimensional echocardiography in chronic animal and clinical studies: a comparison with postmortem examination and magnetic resonance imaging. *J Am Soc Echocardiogr*. 2005;18:1037–1043.
27. Jenkins C, Bricknell K, Hanekom L, Marwick TH. Reproducibility and accuracy of echocardiographic measurements of left ventricular parameters using real-time three-dimensional echocardiography. *J Am Coll Cardiol*. 2004;44:878–886.
28. Caiani EG, Corsi C, Sugeng L, MacEneaney P, Weinert L, Mor-Avi V, Lang RM. Improved quantification of left ventricular mass based on endocardial and epicardial surface detection with real time three dimensional echocardiography. *Heart*. 2006;92:213–219.
29. Mor-Avi V, Sugeng L, Weinert L, MacEneaney P, Caiani EG, Koch R, Salgo IS, Lang RM. Fast measurement of left ventricular mass with real-time three-dimensional echocardiography: comparison with magnetic resonance imaging. *Circulation*. 2004;110:1814–1818.
30. Noble BJ, Borg GA, Jacobs I, Ceci R, Kaiser P. A category-ratio perceived exertion scale: relationship to blood and muscle lactates and heart rate. *Med Sci Sports Exerc*. 1983;15:523–528.
31. Abudiab MM, Redfield MM, Melenovsky V, Olson TP, Kass DA, Johnson BD, Borlaug BA. Cardiac output response to exercise in relation to metabolic demand in heart failure with preserved ejection fraction. *Eur J Heart Fail*. 2013;15:776–785.

32. Bellavia D, Pellikka PA, Al-Zahrani GB, Abraham TP, Dispenzieri A, Miyazaki C, Lacy M, Scott CG, Oh JK, Miller FA Jr. Independent predictors of survival in primary systemic (Al) amyloidosis, including cardiac biomarkers and left ventricular strain imaging: an observational cohort study. *J Am Soc Echocardiogr*. 2010;23:643–652.
33. Quarta CC, Solomon SD, Uraizee I, Kruger J, Longhi S, Ferlito M, Gagliardi C, Milandri A, Rapezzi C, Falk RH. Left ventricular structure and function in transthyretin-related versus light-chain cardiac amyloidosis. *Circulation*. 2014;129:1840–1849.
34. Buss SJ, Emami M, Mereles D, Korosoglou G, Kristen AV, Voss A, Schellberg D, Zugck C, Galuschky C, Giannitsis E, Hegenbart U, Ho AD, Katus HA, Schonland SO, Hardt SE. Longitudinal left ventricular function for prediction of survival in systemic light-chain amyloidosis: incremental value compared with clinical and biochemical markers. *J Am Coll Cardiol*. 2012;60:1067–1076.
35. Koyama J, Falk RH. Prognostic significance of strain Doppler imaging in light-chain amyloidosis. *JACC Cardiovasc Imaging*. 2010;3:333–342.
36. Bellavia D, Pellikka PA, Abraham TP, Al-Zahrani GB, Dispenzieri A, Oh JK, Bailey KR, Wood CM, Lacy MQ, Miyazaki C, Miller FA Jr. Evidence of impaired left ventricular systolic function by Doppler myocardial imaging in patients with systemic amyloidosis and no evidence of cardiac involvement by standard two-dimensional and Doppler echocardiography. *Am J Cardiol*. 2008;101:1039–1045.
37. Koyama J, Ray-Sequin PA, Falk RH. Longitudinal myocardial function assessed by tissue velocity, strain, and strain rate tissue Doppler echocardiography in patients with AL (primary) cardiac amyloidosis. *Circulation*. 2003;107:2446–2452.
38. Ternacle J, Bodez D, Guellich A, Audureau E, Rappeneau S, Lim P, Radu C, Guendouz S, Couetil JP, Benhaiem N, Hittinger L, Dubois-Rande JL, Plante-Bordeneuve V, Mohty D, Deux JF, Damy T. Causes and consequences of longitudinal LV dysfunction assessed by 2D strain echocardiography in cardiac amyloidosis. *JACC Cardiovasc Imaging*. 2016;9:126–138.
39. Phelan D, Collier P, Thavendiranathan P, Popovic ZB, Hanna M, Plana JC, Marwick TH, Thomas JD. Relative apical sparing of longitudinal strain using two-dimensional speckle-tracking echocardiography is both sensitive and specific for the diagnosis of cardiac amyloidosis. *Heart*. 2012;98:1442–1448.
40. Kado Y, Obokata M, Nagata Y, Ishizu T, Addetia K, Aonuma K, Kurabayashi M, Lang RM, Takeuchi M, Otsuji Y. Cumulative burden of myocardial dysfunction in cardiac amyloidosis assessed using four-chamber cardiac strain. *J Am Soc Echocardiogr*. 2016;29:1092–1099.e2.
41. Dorbala S, Vangala D, Bruyere J Jr, Quarta C, Kruger J, Padera R, Foster C, Hanley M, Di Carli MF, Falk R. Coronary microvascular dysfunction is related to abnormalities in myocardial structure and function in cardiac amyloidosis. *JACC Heart Fail*. 2014;2:358–367.
42. Wolsk E, Bakkestrom R, Thomsen JH, Balling L, Andersen MJ, Dahl JS, Hassager C, Moller JE, Gustafsson F. The influence of age on hemodynamic parameters during rest and exercise in healthy individuals. *JACC Heart Fail*. 2017;5:337–346.
43. Harms HJ, Hansson NHS, Kero T, Baron T, Tolbod LP, Kim WY, Frokiaer J, Flachskampf FA, Wiggers H, Sorensen J. Automatic calculation of myocardial external efficiency using a single 11C-tracer and dualacetate PET scan. *J Nucl Cardiol*. 2018. Available at: https://link.springer.com/article/10.1007/s12350-018-1338-0. Accessed October 29, 2018.
44. Harms HJ, Tolbod LP, Hansson NH, Kero T, Orndahl LH, Kim WY, Bjerner T, Bouchelouche K, Wiggers H, Frokiaer J, Sorensen J. Automatic extraction of forward stroke volume using dynamic PET/CT: a dual-tracer and dual-scanner validation in patients with heart valve disease. *EJNMMI Phys*. 2015;2:25.